Defense Technical Information Center Compilation Part Notice

ADP011130

TITLE: Active Structural Acoustic Control as an Approach to Acoustic Optimization of Lightweight Structures

DISTRIBUTION: Approved for public release, distribution unlimited

This paper is part of the following report:

TITLE: Active Control Technology for Enhanced Performance Operational Capabilities of Military Aircraft, Land Vehicles and Sea Vehicles [Technologies des systemes a commandes actives pour l'amelioration des performances operationnelles des aeronefs militaires, des vehicules terrestres et des vehicules maritimes]

To order the complete compilation report, use: ADA395700

The following component part numbers comprise the compilation report:
ADP011101 thru ADP011178

Active Structural Acoustic Control as an Approach to Acoustic Optimization of Lightweight Structures

Dirk Mayer, Bernd Vogl, Holger Hanselka
Otto-von-Guericke-University Magdeburg
Department of Adaptronics
Universitätsplatz 2
39106 Magdeburg, Germany
e-mail: dirk.mayer@mb.uni-magdeburg.de
e-mail: bernd.vogl@mb.uni-magdeburg.de
e-mail: holger.hanselka@mb.uni-magdeburg.de

Conventional approaches to optimizing the acoustic behavior of lightweight structures have mainly been restricted to the concept of *Active Noise Control* (ANC). This concept is aimed to attenuating primary noise sources with secondary controlled noise sources by taking advantage of destructive interference.
However, it is also possible to actively control the vibrating structure using piezoceramic actuators to alter very intensively sound-radiating operating deflection shapes. This approach is referred to as *Active Structural Acoustic Control* (ASAC). The applicability of this concept to real systems is demonstrated by means of a simple model with experimental measurement systems employed in the lower frequency range.
This study focuses on the utilization of a modern measurement technology, i.e. the *Spatial Transformation of Sound Fields* (STSF), which facilitates the determination of important parameters of the vibro-acoustic system at a time. The radiation efficiency is of major importance to the evaluation of the acoustic system behavior. As the lower frequency range is considered, the dynamic system behavior is determined by means of the *Experimental Modal Analysis* (EMA).
The results of this study show the radiation efficiency of the unregulated and of the actively controlled system.

1. INTRODUCTION

The adaptronic approach is aimed at combining mechanical systems by incorporating integrated actuators and sensors into the structure and by controlling the whole complex to obtain the desired adaptive response to physical effects which may be caused by external impacts. To this end, it is necessary to know the exact description of the mechanical system, choose appropriate actuator and sensor systems, and design the control algorithm on the basis of a predefined objective function.
For many applications in the industry approaches are employed which focus on the utilization of alternative materials to obtain a more economical and efficient design.
Often also aspects of convenience play a role.

The present study is not aimed at developing new optimization methods, but the authors want to demonstrate the potentials of adaptive systems by means of a simple experimental setup. Considering the intensified use of lightweight construction in future applications, a rectangular plate was investigated which was very thin compared to its dimensions. The material was steel, although composites with integrated piezoceramics as actuators are intended to be used for further investigations. In addition, this study was restricted to the lower frequency range where the low modal density makes efficient control less difficult. The merely passive approach of sound absorbing materials (sandwich panels) was not considered.
Future activities should concentrate on the efficiency of adaptive systems in the higher frequency range where deterministic model descriptions are not possible. An appropriate approach based on *Statistical Energy Analysis* (SEA) would facilitate investigations of the structural behavior at a high modal density.
On the way to improve the acoustic features of mechanical structures novel vibro-acoustic phenomena appear. Basically, it is possible to give a theoretical description of the sound field induced by known structure-borne sound within the lower frequency range (Finite Element Method, Boundary Element Method), but in reality deviation problems occur which require profound knowledge. In contrast to more conventional methods, such as *Active Noise Control* (ANC), which focuses on attenuating primary noise sources with secondary controlled noise sources (loudspeakers) by taking advantage of destructive interference, this study was aimed at altering structural properties. This method is referred to as *Active Structural Acoustic Control* (ASAC, [1]). It is applied to actively manipulate the vibrating structure by means of suitable actuators in order to obtain a specific repercussion onto the intensively sound-radiating structural behavior.
The present investigations were mainly based on experiments and demonstrate the chances offered by adaptive systems. An established measurement method is described facilitating important conclusions about the real vibro-acoustic behavior of a simple experimental setup.

2. EXPERIMENTAL SETUP

A wooden box with the overall dimensions of 930 x 635 x 620 mm was designed to investigate the efficiency of active sound-reducing measures. The wall material consisted of 20 mm thick glazed insulation pressboard. The box, which was open to the upper side, was covered by a steel frame holding the steel sheet in position. Hence, an efficient air cushion of 900 x 600 x 650 mm was built up below the plate. The plate dimensions in the fixing frame were 905 x 605 x 1 mm. A flexible rubber material was used between the two frame components.

Paper presented at the RTO AVT Symposium on "Active Control Technology for Enhanced Performance Operational Capabilities of Military Aircraft, Land Vehicles and Sea Vehicles", held in Braunschweig, Germany, 8-11 May 2000, and published in RTO MP-051.

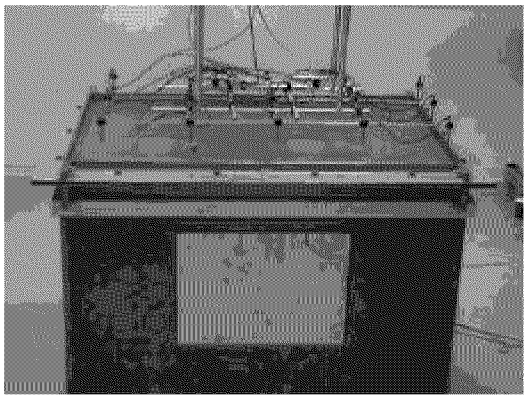

Fig. 2.1 Experimental Setup

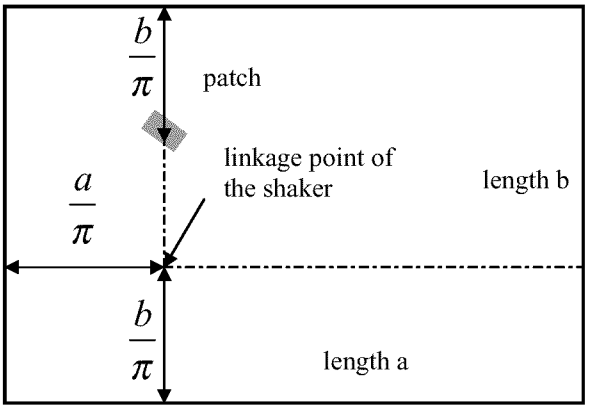

Fig. 2.2 Excitation Points

Primary excitation of the plate was caused by an electrodynamic shaker screwed to the bottom inside the wooden box. The π-th fraction of the surface dimensions was chosen as the exciter place in order to suggest as many eigenmodes as possible at a time. For superposition of a controlled secondary oscillation a piezoceramic patch (50 x 25 x 0.25 mm) was mounted to the bottom side of the plate opposite to the shaker position (see Fig. 2.2).
To measure the sound radiation of the plate above the wooden box, the *Spatial Transformation of Sound Fields* (STSF) measuring system of Brüel & Kjaer was used. The employed microphone array is presented in Fig. 2.1. Theoretical foundations and possible results of this measuring method are detailed in Chapter 4.

3. PRELIMINARY INVESTIGATIONS

To investigate in a first approximation the relationship between structural dynamics (structure-borne sound) and the resulting sound field (airborne sound) the steel sheet was subjected to a dynamic examination. By means of the CADA-X modal analysis software of LMS the deflection modes with their corresponding resonance frequencies were determined experimentally in the frequency range of 0 to 250 Hz. The following results were obtained:

No.	Eigenmode	Frequency [Hz]
1	(2,1)	28.2
2	(1,1)	29.1
3	(1,2)	37.9
4	(3,1)	48.0
5	(2,2)	49.7
6	(3,2)	66.6
7	(4,1)	68.6
8	(1,3)	78.3
9	(4,2)	87.9
10	(2,3)	90.5
11	(5,1)	96.9
12	(3,3)	105.5
13	(5,2)	114.9
14	(4,3)	-
15	(1,4)	126.8
16	(6,1)	132.8
17	(2,4)	141.2
18	(6,2)	152.3
19	(5,3)	156.8
20	(3,4)	158.5
21	(7,1)	173.3
22	(4,4)	180.4
23	(6,3)	-
24	(1,5)	192.6
25	(7,2)	194.4
26	(2,5)	205.9
27	(5,4)	208.6
28	(8,1)	220.6
29	(3,5)	223.3
30	(7,3)	-
31	(6,4)	-
32	(8,2)	241.6
33	(4,5)	246.5

Table 3.1 Results of the Modal Analysis

The frequency resolution of this measurement was 0.195 Hz. The plate was divided into 19 x 13 measuring points (247 frequency responses). Measurement was performed twice to obtain as many eigenmodes as possible. In the first test, the shaker was mounted to the exciter point described above, whereas in the second test it was arranged in th center of the plate.
As can be seen, a strong coupling occurred between the contained air cushion and the plate resulting in a displacement of the (1,1)-mode. The measured damping amounted to approx. 10% (attenuation of the (2,1)-mode was approx. 3.5 %).
The thickness of the steel sheet (d=1 mm) led to a high modal density even in the low frequency range and hence deterministic methods reached their limits very soon. For higher frequency investigations an approach based on the *Statistical Energy Analysis* (SEA) is recommended to describe the structural dynamic behavior.
Then the frequency response, i.e. the ratio of sound pressure with reference to the initiated force, was determined and compared with the mechanical frequency response of the plate (Fig. 3.1).
To measure the sound pressure, a microphone was arranged above the plate at the same distance (approx. 0.5 m) as that chosen for the control described in Chapter 5. Hence, the error signal of the non-controlled state measured later could be obtained in advance.
The "acoustic" frequency response (FRF between sound pressure and force), which was in qualitative agreement to the autopower spectrum of the sound pressure, revealed a marked increase in the effective sound pressure measured in the frequency ranges of 80 to 100 Hz and 170 to 210 Hz compared to the mean sound pressure level (Fig. 3.2).

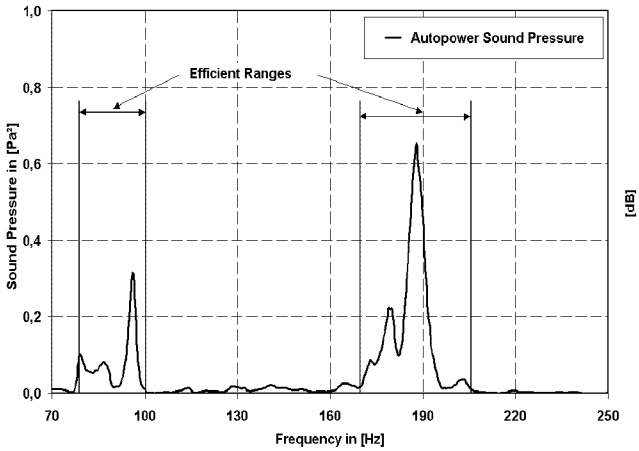

Fig. 3.1 Frequency Response Functions

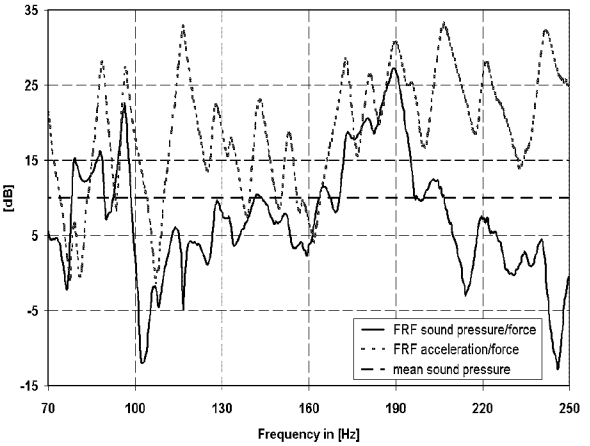

Fig. 3.2 Autopower Spectrum Sound Pressure (Linear)

The control approach which was used thereafter, was mainly aimed at minimizing the mean power of the error signal and yielding good results, in particular for these frequency ranges.
To facilitate a vibro-acoustic evaluation of the overall system, a characteristic parameter was introduced, i.e. the radiation efficiency ζ_{rad}.

Determination of the Radiation Efficiency ζ_{rad}

Radiation efficiency is defined as the ratio of the radiated power P_{rad} which is responsible for the audible airborne sound and the active power P_{in} applied to the plate by the primary vibration source [2]. The following equation leads to this characteristic:

$$\zeta_{rad} = \frac{P_{rad}}{P_{in}} \; . \tag{1}$$

The input power (active power) is calculated from the real part of the complex cross power spectrum of the oscillating velocity and the exciter force:

$$P_{in} = Re\left\{F \cdot v^{*}\right\} . \tag{2}$$

This variable was determined experimentally by using an impedance head at the shaker linkage point.
The radiated sound power results from the product of the active sound intensity and the crossed plate area:

$$P_{rad} = \iint_{A} \vec{I}_A d\vec{A} \; . \tag{3}$$

4. DETERMINATION OF THE RADIATED SOUND POWER

Determination of the radiated sound power of the plate requires the active intensity on its surface be established. To this end, the well-known method of *Nearfield Acoustic Holography* (NAH, [3]) was used. Major steps are described below to draw a complete picture of the calculations.
It is assumed that the sound pressure distribution in a level $z=z_1$ parallel to the radiating plate surface $z=z_0$ is known, for instance through measuring. Hence, a complex spectrum is obtained in the frequency domain:

$$p(x,y,\omega)\big|_{z=z_1} . \tag{4}$$

Using the spatial, two-dimensional Fourier transform, we obtain a corresponding spectrum in the complex variable domain:

$$p'(k_x,k_y,\omega)\big|_{z=z_1} , \tag{5}$$

where the variables k_x and k_y represent the components of the wave vector in the x- and the y- direction.

It is generally known that:

$$\left|\vec{k}\right|^2 = {k_x}^2 + {k_y}^2 + {k_z}^2 = \left(\frac{\omega}{c_0}\right)^2 . \tag{6}$$

As the velocity of sound in the air is defined to be approx. 343 m/s, the third component of the vector can be calculated. Then the sound pressure distribution within the complex variable domain on the plate surface is computed through:

$$p'(k_x,k_y,\omega)\big|_{z=z_0} = e^{-jk_z(z_1-z_0)}\, p'(k_x,k_y,\omega)\big|_{z=z_1} \tag{7}$$

The sound pressure spectrum on the plate surface can be calculated by means of re-transformation using the inverse spatial Fourier transform.
With this method the sound pressures in other levels are also available.
The normal velocity on the plate surface is computed through gradient formation, yielding again a complex spectrum:

$$\vec{v}_z(x,y,z,\omega) = -\frac{1}{j\omega\rho_0}\nabla p(x,y,z,\omega) . \tag{8}$$

Using the velocity and the pressure, the active sound intensity can be computed through the following expression that marks the active power flow:

$$\vec{I}_A = Re\left\{p^* \vec{v}\right\} \tag{9}$$

The radiated active sound power of the plate is obtained by integration over that plate area according to Equation (3). Then the radiation efficiency can be calculated following Equation (1) and Equation (2).

Regarding this *Nearfield Acoustic Holography*, measurements were based on the Brüel & Kjaer's *Spatial Transformation of Sound Fields* (STSF). With this approach the pressure spectrum was only recorded at discrete points in one level and only in a confined area. Hence, calculations require numerical methods (*Fast Fourier Transform*, FFT) and special windows filtering methods be applied to the data.
Upon evaluation of the readings also distant variables (e.g. radiation pattern) are available in addition to the near field variables.

5. IMPLEMENTATION OF ACTIVE MEASURES

The investigated lightweight construction structures of thin steel sheet are mainly used in aircraft construction and in the automotive industry. Hence, the disturbances in the overall structure are often caused by motors and other units. Consequently, the disturbance is deterministic and an adaptive counter-control (adaptive Feed-Forward Control) can be used. This principle has already been applied to practice, and was also used for this experiment.
The required reference signal for a narrow-band disturbance can be obtained either from the corresponding motor speed signals or from a component not affected by active measures, e.g. by means of acceleration sensors at an engine mount.
The system should work adaptively to be able to respond to changes in the characteristics of the disturbance or in the characteristics of the structural dynamic system. The performance is kept constant.

To this end, an error sensor, e.g. a measurable variable, is required to evaluate of the performance of the adaptive control system.
A microphone was used which was arranged at a distance of about half a meter above the center of the plate surface.
Adaptive signal processing was implemented as a digital filter system [4]. The actuator signals were obtained through filtering by means of an adaptive digital filter; the coefficients of the filter had been adapted using the so-called *Filtered-X-LMS* algorithm.
Figure 5.1 depicts the block diagram of the system. *W(z)* is the adaptive FIR digital filter (FIR: *Finite Impulse Response*) and *P(z)* represents the transfer function from the disturbance source to the microphone, *S(z)* is the transfer function from the actuator to the microphone and $\hat{S}(z)$ describes a model of this transfer function which had to be generated prior to test start. Again, an adaptive FIR filter is used to this end.
The model of the path *S(z)* is necessary to ensure the convergence of the filter coefficients *w* of the adaptive filter, following the known algorithm:

$$w(n+1) = w(n) + \mu \underline{x}'(n)e(n) \tag{10}$$

In contrast to most of the filter systems where the assembler language is used, the *MATLAB/Simulink* environment was employed here to ensure good readability as well as simple testing and changing. By applying the *dSpace* rapid prototyping system such models can be run on a signal processor. Figure 5.2 demonstrates the completed, simple Simulink model.
It still facilitates on-line adaptation of the so-called secondary path *S(z)*, where the signal is superposed low-power noise and the identification prior to the test start is updated.

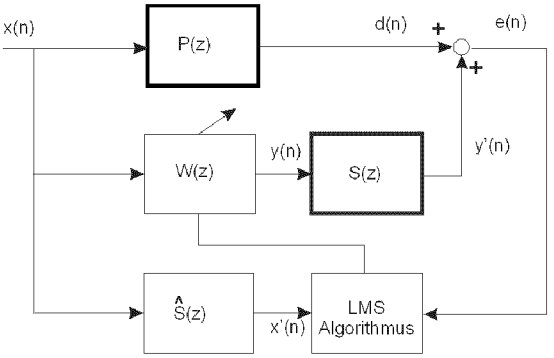

Abb. 5.1 Adaptive Feed-Forward Control System

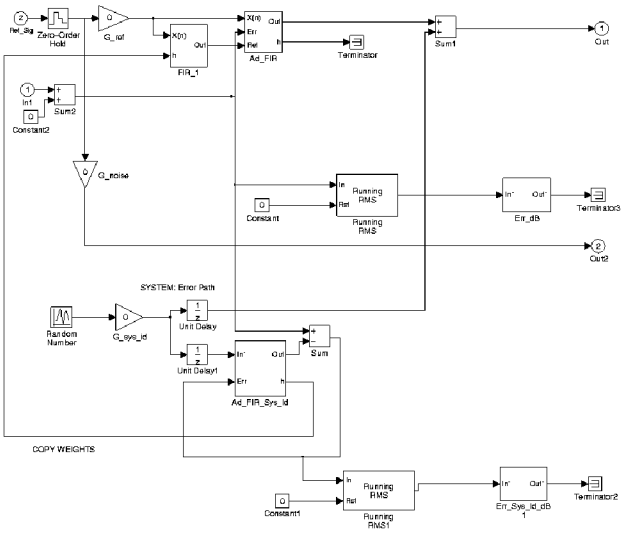

Fig. 5.2 *MATLAB/Simulink* Model

Hence, *W(z)* and the required model $\hat{S}(z)$ are adaptive which is an interesting property of control systems in structural dynamics. In particular in lightweight construction structures, this property may alter either the characteristics of the disturbance or the mechanical transfer functions between actuators and sensors, e.g. by loading of the structure or by changing of the boundary conditions, such as the temperature.
The adaptive feed-forward control system was first subjected to harmonic investigations under different sound radiating frequencies of the plate.
This paper presents two experiments which were carried out at a signal frequency of f=191 Hz. For this frequency a large signal was measured in the sound pressure spectrum at the microphone.
Figure 5.3 shows the progression of the error and the actuator signal when the adaptive feed-forward control is switched on, with all coefficients of the adaptive filter *W(z)* reset before.
To test the adaptability of the system to changed boundary conditions an additional magnetic weight with the mass m = 0.1 kg was arranged in the actuator position on the plate. Figure 5.4 shows how the adaptation algorithm follows the actuator signal when the weight has been placed. The overshoot of the error signal results from the noise occurring at the moment when the weight was placed onto the plate.
In the following experiments this controller was used for both harmonic and broadband excitation. In both cases it received reference signals from the generator.

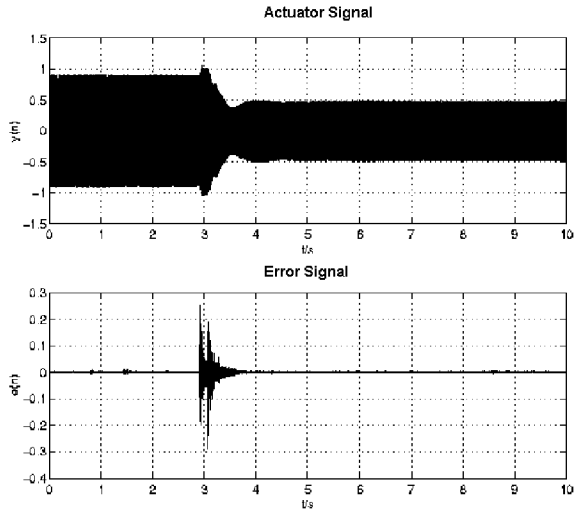

Fig. 5.3 Adaptation of the Feed-Forward Control

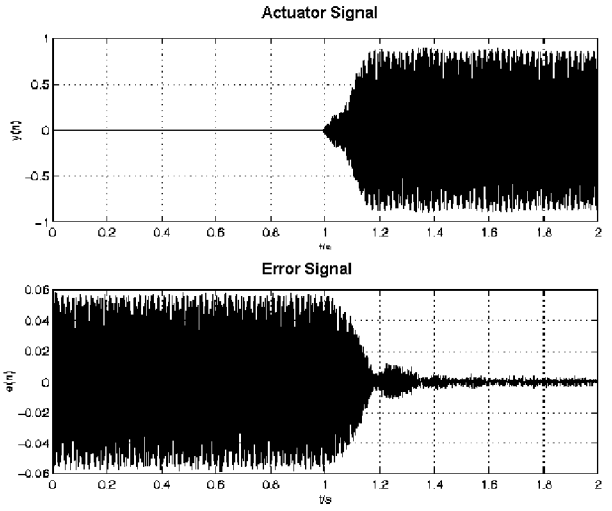

Fig. 5.4 Adaptation of the Actuator Signal to changing mechanical Conditions

6. RESULTS

This chapter is divided into sections to ensure precise analysis of the sound field and of the plate mechanics for harmonic and broadband excitation. The results of the STSF measurement are important to the understanding of the physical phenomena. The description of the vibro-acoustic parameter ζ_{rad} involves a comparison of the non-controlled actual state with the regulated state and provides an explanation of the changed radiation pattern. In addition, the properties of the actuators (PZT patches) used are detailed.
In an harmonic experiment the efficiency of the overall active system and the possibilities of measuring technologies were tested.
The results of this experiment served to evaluate the potential of the overall active system under the conditions of broadband excitation considering the parameters determined above.

Results of Harmonic Excitation

The plate was subjected to harmonic excitation at 96.9 Hz ((5,1)-eigenmode). The distribution of the normal surface velocity on the plate obtained by performing a STSF measurement is represented in Fig. 6.1. The minimum resolution of the STSF measurement is 1 Hz, and was limited to 2 Hz for reasons of the measuring period. A comparison of the plate movement with the results of the experimental modal analysis at resonance frequencies reveals similar vibrating forms. The result was the (5,1)-eigenmode of the plate causing high amplitudes in the sound pressure spectrum. In a simplified form this can be attributed to the oscillating mode of motion which assumes an odd-odd eigenmode where sources and depressions cannot be compensated for with regard to sound intensity (no acoustic short circuit).

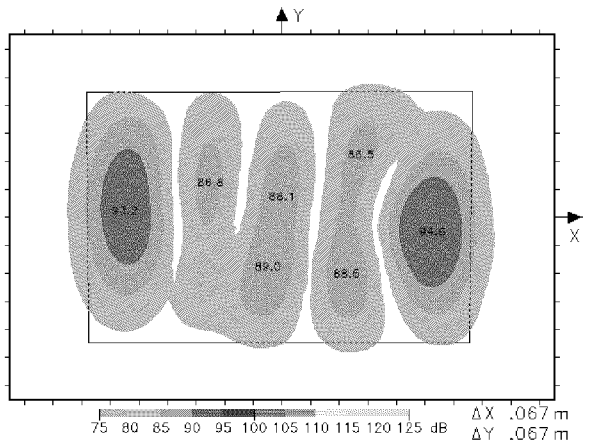

Fig. 6.1 Normal Velocity at 98 Hz; Non-Controlled

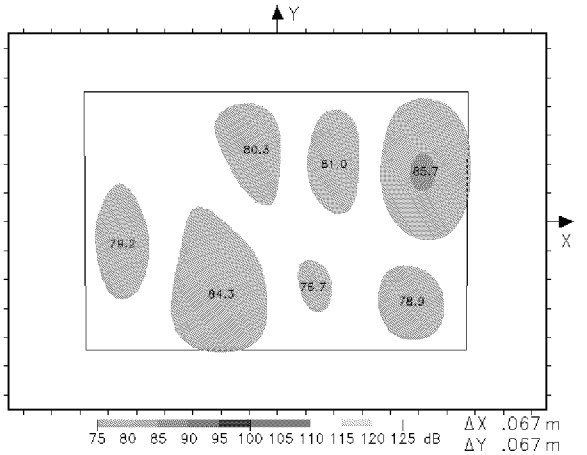

Fig. 6.2 Normal Velocity at 98 Hz; Controlled

To minimize sound radiation the adaptive controller described above was inserted. With the convergence of the filter coefficients a decrease in power of the microphone signal by approx. 20 decibel was obtained. A changed operating deflection shape occurred as shown in Fig. 6.2.
As clearly can be seen, the velocity amplitudes decreased. This size is correlated to the sound radiation in harmonic investigations. As the surface velocity could not be taken into consideration when calculating the sound pressure within the

far field basically (broadband), the active intensity for both the non-controlled and the controlled structure was measured (Fig. 6.3 and 6.4).

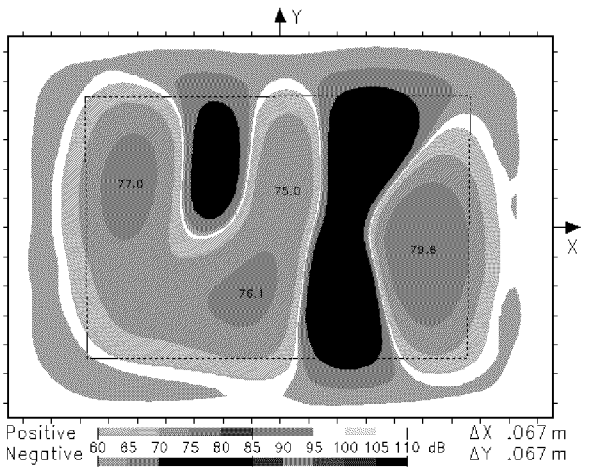

Fig. 6.3 Active Intensity at 98 Hz; Non-Controlled

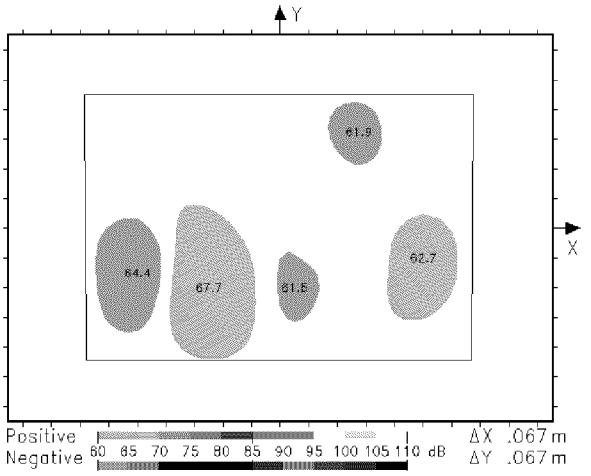

Fig. 6.4 Active Intensity at 98 Hz; Controlled

This variable is important to sound radiation into the far field and exhibits a dramatic drop caused by the adaptive controller. In addition, the figure shows that the decrease in intensity the force transmitting position of the shaker is rather small.

Results of Broadband Excitation

For this test the system was excited by white noise with a bandwidth of 70 to 250 Hz. The radiation efficiency ζ_{rad} described above was used to illustrate the radiation pattern of the investigated system already is used. By means of the measurement technology mentioned above, this parameter could be determined for broadband excitation.
First the performance of piezoceramic actuators (PZT patches) was analyzed with regard to an efficient broadband regulation. As can be clearly seen from the curve of the electrical active power incorporating a PZT patch with the dimensions of 50 x 25 x 0.25 mm (linkage factor neglected), the power increase follows the frequency and is very small in the frequency range considered here. As a result more energy and hence more or thicker PZT patches need be applied to obtain a better radiation compensation.
The incorporated electrical power of piezoceramics is determined by measuring the cross power spectrum of current and voltage.

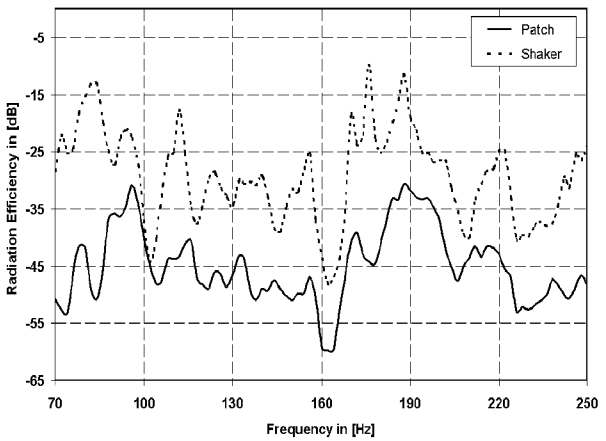

Fig. 6.5 Incorporated Active Power of a PZT Patch

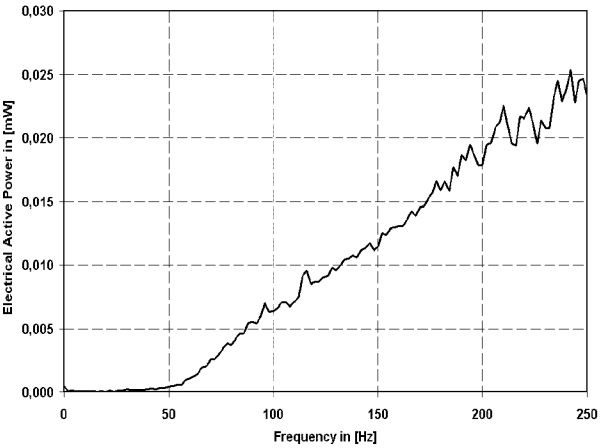

Fig. 6.6 Radiation Efficiency of Patch and Shaker; Non-Controlled

The radiation efficiency ζ_{rad} is obtained from the determined radiated power and the imported power of the exciters following Equation 1 (Fig. 6.6).
The distance between the two curves are caused by the different measuring methods of the input power for both the shaker and the patch. Only the electrical efficiency was taken into consideration when determining the input power of the patch. The result was a lower radiation efficiency caused by coupling losses of the mechanical structure which are still unknown. Hence, a vertically downward displacement occurred.

Considering the error signal for the measurement of the regulated system (Fig. 6.7), it turns out that the signal markedly decreased in various frequency ranges, whereas in other ranges it remained unaffected or was even extended. However, the total power decreased across all frequencies by 4.63 decibels because the adaptation algorithm caused a minimization of the total power of the microphone signal.

The limited efficiency and the restriction to a small range of the stimulated spectrum were mainly attributed to the following conditions:

- The microphone is not arranged in optimum position; several microphones might have been necessary.
- The PZT patch was not arranged in optimum position either, hence, its efficiency at low frequencies was extremely low and several piezoceramics in optimized positions might have been necessary.

Thereafter, the above method was used to determine the radiation efficiency for both adaptively controlled and non-controlled structures to analyze also the influence exerted by secondary excitation (by PZT patch) on the radiation behavior (Fig. 6.8).
As can be seen, the vibro-acoustic parameter improved in those ranges where the error signal of the adaptive controller was reduced and the radiation characteristics of the plate changed as desired.

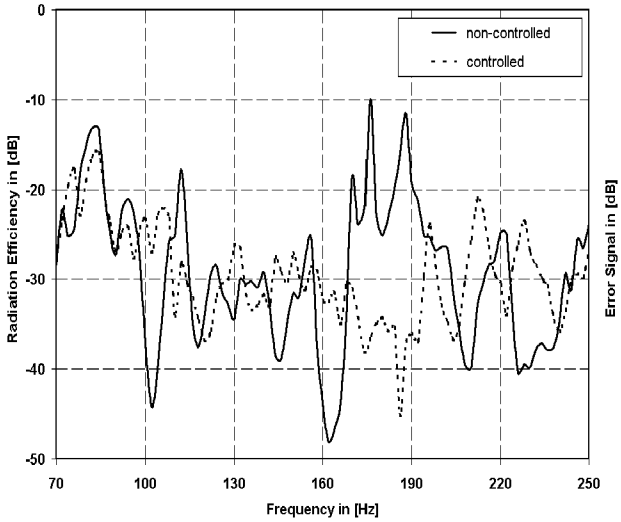

Fig. 6.7 Error Signal at the Microphone

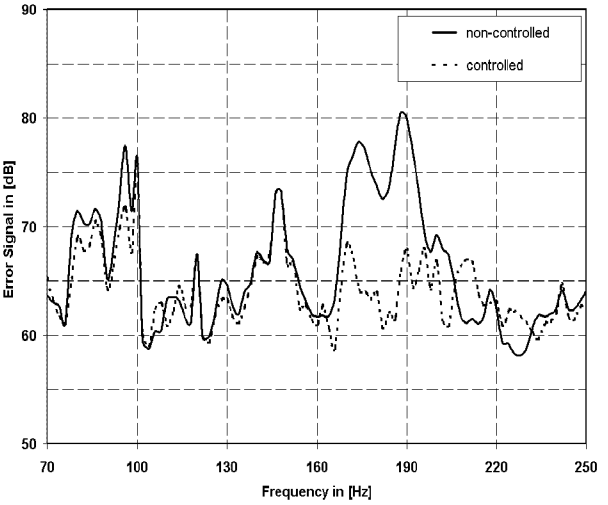

Fig. 6.8 Radiation Efficiency of Primary Excitation

7. CONCLUSION AND PROSPECTS

An active lightweight construction structure was examined by means of a basic experiment. It revealed that the vibro-acoustic behavior of the active system can be evaluated using the radiation efficiency. A method for calculating this parameter was presented and verified experimentally.
However, improvements were possible to an extent only when an adaptive feed-forward control was used which comprised only one piezoceramic patch as an actuator and one microphone as an error sensor.
Hence, future investigations must be aimed at optimizing the number and positions of actuators and sensors. In addition, such investigations should be conducted in the higher frequency range. The results would help to substitute damping materials as mentioned above. These studies will finally serve as a basis for analyzing real lightweight construction structures, e.g. in aviation and the automotive industry.

8. REFERENCES

[1] C.R. Fuller, S.J.Elliot, P.A. Nelson, *Active Control of Vibration,* Academic Press, London, 1996

[2] L. Cremer, M. Heckl, *Körperschall: Physikalische Grundlagen und technische Anwendungen*, 2. Völlig neubearbeitete Auflage, Springer, 1996

[3] J.D. Maynard, E.G. Williams, Y. Lee: "Nearfield acoustic holography. 1. Theory of generalized holography and the development of NAH" J. Acoust. Soc. Am. 78 (4), 1395-1412, (1985)

[4] S.E. Kuo, D.R. Morgan, *Active Noise Control Systems*, Wiley 1996